Zernike wavefront sensor (ZWFS) development for Low Order Wavefront Sensing (LOWFS)

Xu Wang, Fang Shi, J. Kent Wallace
Jet Propulsion Laboratory, California Institute of Technology, Pasadena, CA 91109-8099

ABSTRACT

ZWFS is known to be photon noise optimal for measuring low order aberrations. Recently, ZWFS was selected as the baseline LOWFS technology on WFIRST for its sensitivity, accuracy, and its ease of integration with the starlight rejection mask. In this paper, we present the development of ZWFS sensor, including the algorithm description, sensitivity analysis, and some early experimental model validation results from a fabricated ZWFS phase mask on a stand-alone LOWFS testbed.

Key words: Wavefront sensing, Zernike phase contrast, WFIRST, LOWFS

1. INTRODUCTION

Wide-Field InfraRed Survey Telescope (WFIRST) was the top-ranked large space mission in the New Worlds New Horizons Decadal Survey of Astronomy and Astrophysics in 2010. WFIRST observatory demands tens of picometers optical wavefront stability to achieve the required level of starlight suppression with ~1e-9 coronagraph contrast. The LOWFS/C subsystem work with the primary WFIRST coronagraph architecture called Occulting Mask Coronagraph (OMC) that combines two operating modes: Shaped Pupil Coronagraph(SPC) and Hybrid Lyot Coronagraph (HLC). These two modes share the same LOWFS/C hardware. ZWFS sensor is the sensor (eye) of this LOWFS/C system.

The paper is structured as follows. Section 2 describes the ZWFS analysis, including modeling scheme, performance metrics, and some study results. Section 3 presents the design detail of a ZWFS test mask and the comparison between modeling prediction and measurement data. The paper ends with a conclusion in Section 4.

2. ZWFS ANALYSIS

2.1 ZWFS modeling

Figure 1 illustrates the concept of the Zernike wavefront sensor in the context of an astronomical instrument. The wavefront error (WFE) is the wavefront phase variation at the entrance pupil plane. An imaging system forms a stellar image with intensity distribution that depends on the WFEs and intensity distribution in the pupil. A transparent phase mask is placed at the focal plane where the star image is formed, introducing a phase change for the central part of the star image. The light that passes through this small phase mask acts as a reference wavefront, and interferes with the light passing outside the phase disk that contains the information on wavefront aberrations. The interfered light is reimaged to another pupil, where a camera records the

*xu.wang@jpl.nasa.gov; phone: 818-393-0229; fax: 818-393-4357; http://www.jpl.nasa.gov

intensity pattern that depends on the input wavefront aberration (phase error). The exact intensity encoding of the WFE depends on various design parameters[1].

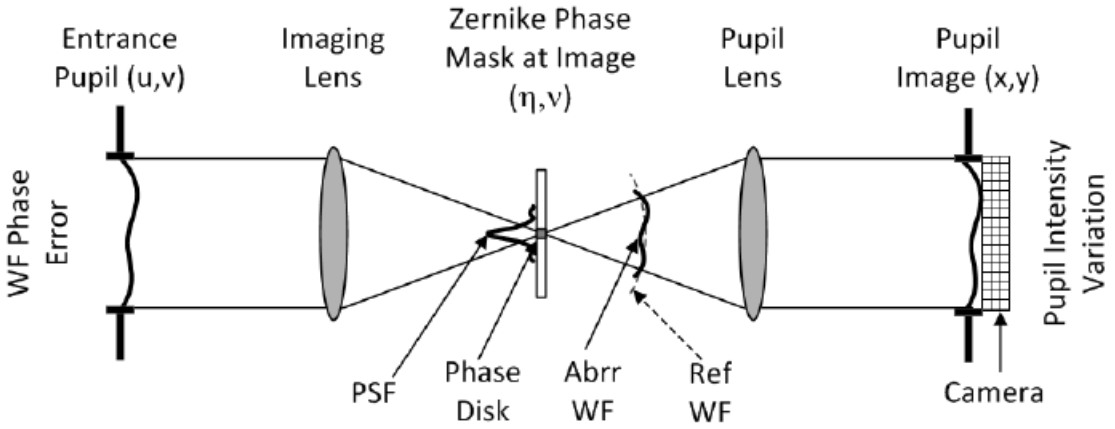

Figure 1 Illustration of Zernike wavefront sensor concept. Lenses are used here to represent the optics between entrance pupil, imaging plane, and re-imaged pupil plane.

To analyze the performance of ZWFS, we developed an end-to-end diffraction model, utilizing a semi-analytical method (SAM) [2]. Figure 2 shows the ZWFS modeling process (using HLC configuration as an example). The interference of ZWFS turns the wavefront phase error at entrance pupil into an intensity variation at ZWFS's camera, which mimics the phase error map when the DC components from the complex diffraction of the pupil geometry, DMs setting, and phase mask are removed. To model the ZWFS performance, a set of baseline modeling parameters that are consistent with the current coronagraph design have been used to better represent the real system. For photometry, a G type star is used for rejected starlight and the star magnitude varies from Mv=0 to Mv=8. The total effective system transmission is 0.24 which takes into account all of the WFIRST coronagraph optical element throughputs. The ZWFS pupil sampling is 16x16 pixels, which was chosen to optimize the sensor signal-to-noise ratio (SNR) and minimize WFE modes cross-talk (more details seen in Section 3). We assume a E2V CCD39 chip with 4 e- read out noise, 1 e- dark noise at 1 kHz frame rate, and about 80% to 87% quantum efficiency (QE) covering 128 nm spectral band centered at 561 nm

Our ZWFS model has three configurations: (1) the simple phase disk configuration where the ZWFS focal plane mask is a $\pi/2$ phase disk of ~1.22 λ/D diameter with the PSF generated from the WFIRST pupil (2) the HLC configuration where the Focal Plane Mask (FPM) is the HLC occulter and both DMs have special patterns that are an integral part of the HLC design for WFIRST coronagraph. (3) the SPC configuration where an optimized shaped pupil mask creates a unique PSF with areas of high starlight cancelation. The FPM is a bow-tie shaped occulter with a $\pi/2$ phase disk of size ~1.22 λ/D in the center.

2.2 Performance metrics

An important ZWFS performance metrics is the noise equivalent sensing error. It measures the sensor performance when the photon and detector noise are present. We analyze ZWFS sensor noise performance as follows:

1) Generate the ZWFS image with no aberrations using ZWFS model
2) Added photon and detector noise to this image in 100 random realizations
3) For each realization, generate ZWFS differential image and reconstruct the

corresponding Zernike coefficients. Since the image has no WFE, the sensed WFE is the noise equivalent sensing errors

4) Take the average of the 100 random realizations of sensing error to obtain the mean RMS of tilts (Z2, Z3) and OPD (Z4 to Z11) sensing errors to find the noise equivalent sensing error. Convert the noise equivalent tilt to noise equivalent line of sight angle

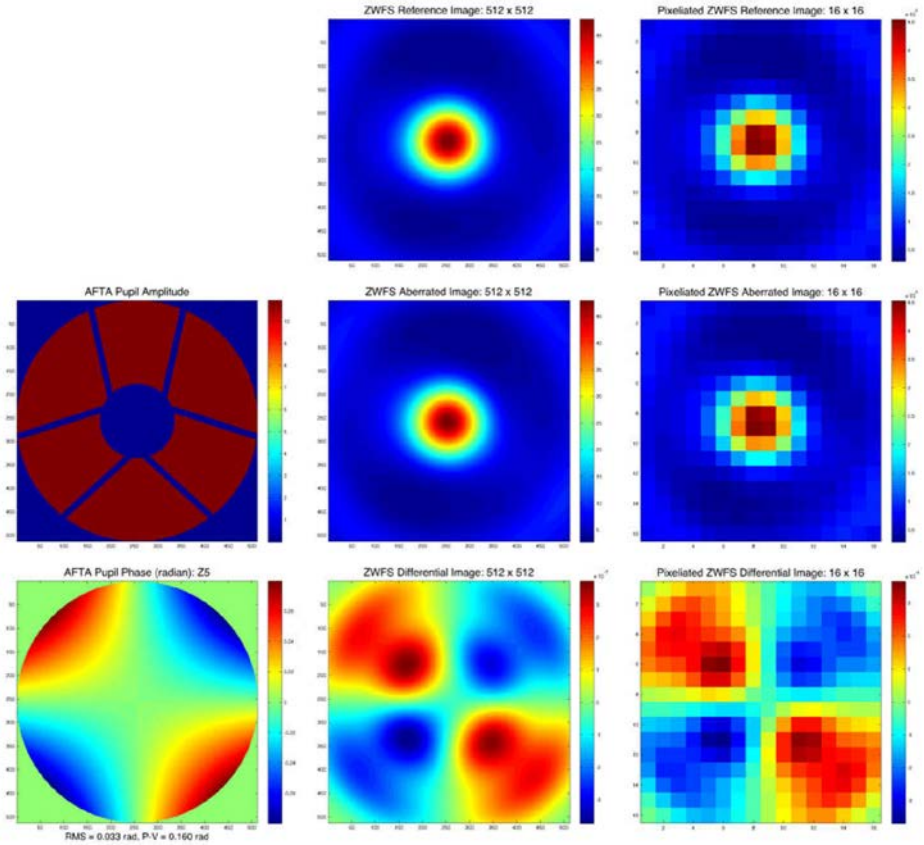

Figure 2 Example images of ZWFS modeling process using the HLC configuration. The images on the left column are the amplitude and phase error at WFIRST entrance pupil. Here the phase error is 45 degree astigmatism (Z5). The images in middle column are, from top to bottom, the high resolution ZWFS reference (no phase error) image, the aberrated image, and the differential image. The images on the right column are, from top to bottom, the corresponding pixelated (16x16 pixels) reference, aberrated, and differential images. The differential images mimic closely the phase error input.

Figure 3 shows the noise equivalent LoS angle and noise equivalent sensing error for the simple phase dimple model. Notice that the ZWFS noise sensing error dominates the photon noise with sensing errors and star magnitudes following a power law curve. Only for fainter stars of Mv > 7, does the noise performance curve begin to deviate from this power law, as the detector noise starts to dominate. It is important to emphasize that this noise performance curve is evaluated at camera readout rate of 1 kHz. For slowly drifting low order WFE, the sensor performance can be improved through image averaging, which is equivalent to increasing the stellar brightness. For example, if we average 1000 camera images (equivalent read out rate of one frame per second), the 0.5 nm sensing error from an Mv = 5 star will be reduced to 16 pm.

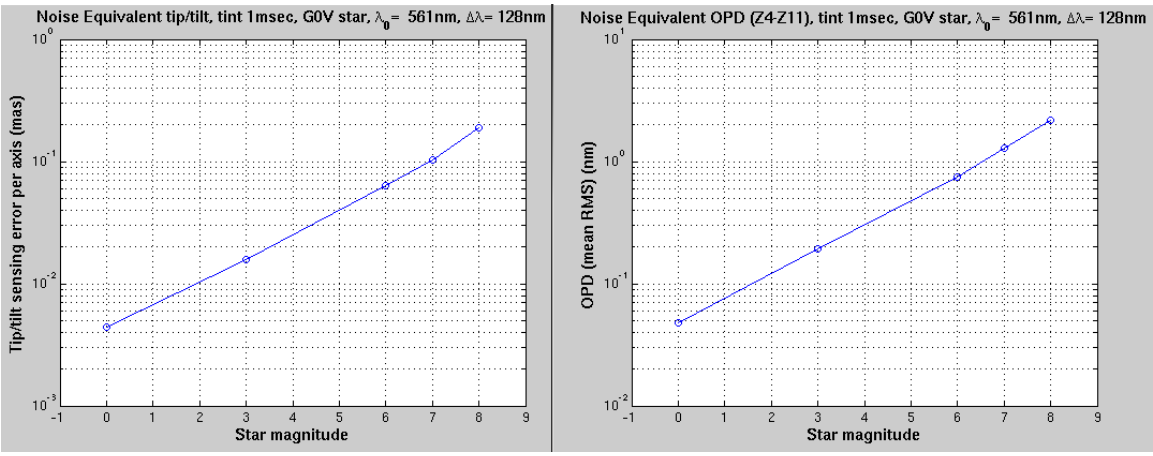

Figure 3 ZWFS noise performance for a simple Zernike phase disk configuration with the ZWFS camera running at 1 kHz frame rate. The plot on the left is the noise equivalent angle and plot on the right is that of noise equivalent low order WF sensing error.

2.3 ZWFS analysis

This section describes mew ZWFS analysis. Reference[1] describes earlier results.

2.3.1 Phase dimple diameter

Figure 4 shows the ZWFS performance with different sized phase dimples. The best noise performance is at 1.22 λ/D diameter, ~half of the Airy disk size.

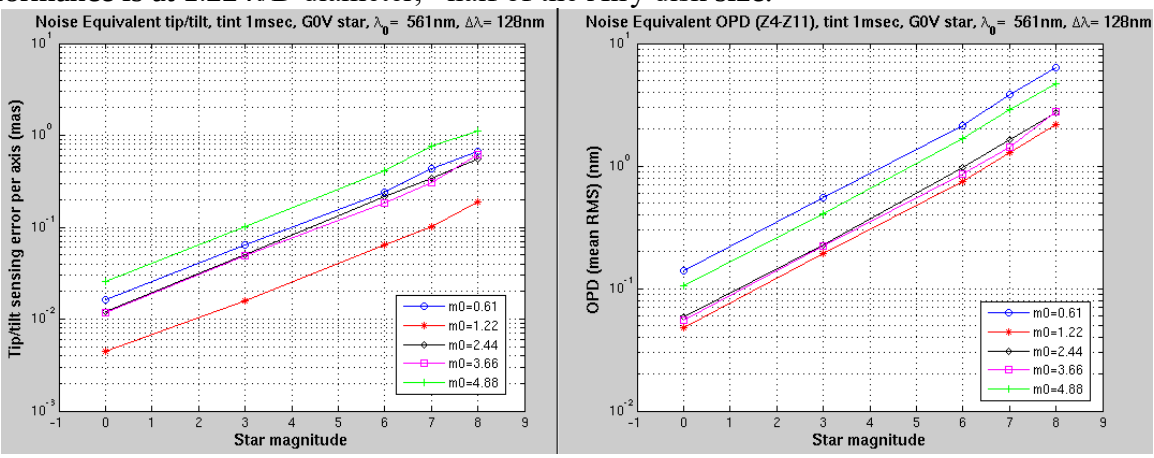

Figure 4 ZWFS noise performance versus phase dimple size, where m0 is the multiple of λ/D. The plot on the left shows the effect on noise equivalent angle, and the plot on the right is that of low order WFE sensing error.

2.3.2 Phase dimple depth

Figure 5 shows the ZWFS performance with the phase dimple at different phase depths. The optimal phase depth with the best noise performance is around 0.5π.

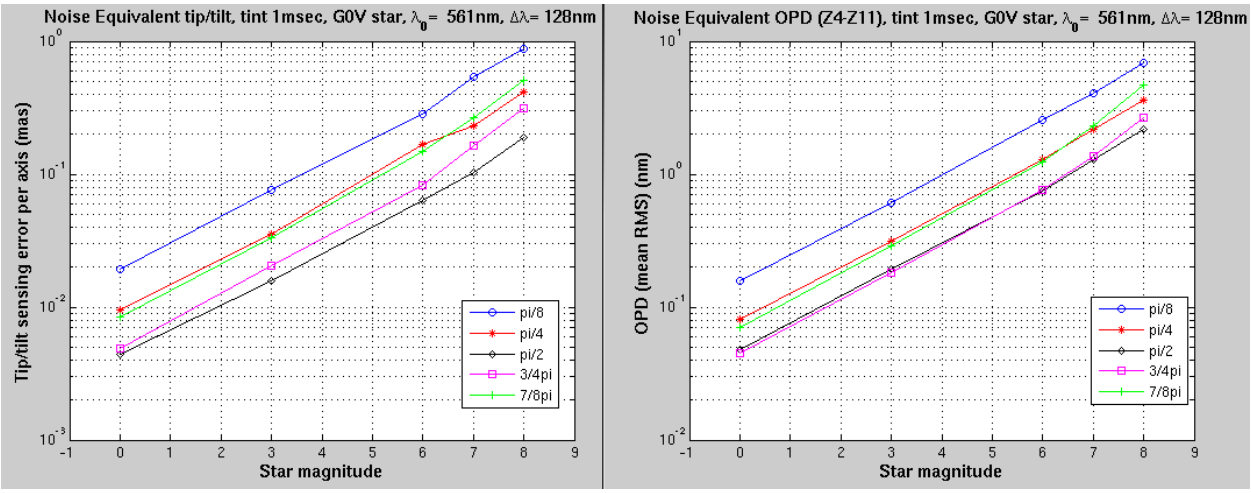

Figure 5 ZWFS noise performance on phase depth. The plot on the left shows the effect on noise equivalent angle, and the plot on the right is that of low order WFE sensing error.

2.3.3 Wavefront correction working range
We estimated the maximum correctable WFE by
1)Applying an original WFE at the pupil with known RMS
2)Sensing this WFE using ZWFS sensor and extracting the corresponding Zernike coefficients
3)Removing the sensed WFE out of original WFE to get the residual WFE
4)Sensing this residual WFE using ZWFS sensor and extracting the Zernike coefficients again
5)Iterating the step2 to 4 to determine the maximum WFE that can be corrected/minimized

Figure 6 shows the WFSC result.The maximum correctable WFE RMS is about half-wavelength.

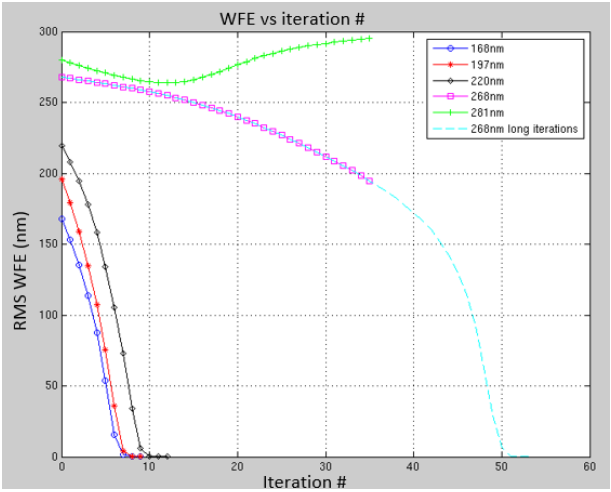

Figure 6 ZWFS&C analysis. Maximum correctable WFE RMS is about half-wavelength.

3. ZWFS MODELING VS MEASUREMENT

We validated the ZWFS modeling against experimental data from a ZWFS phase mask in the HLC configuration.

3.1 HLC configuration

The HLC phase plate at the focal plane combines the coronagraph phase profile and the ZWFS phase dimple. It creates a common mode on WFE sensing for both coronagraph path and LOWFS path. Figure 7 shows an HLC mask phase profile where the center flat portion is the ZWFS phase dimple and the annular rings are for the coronagraph path.

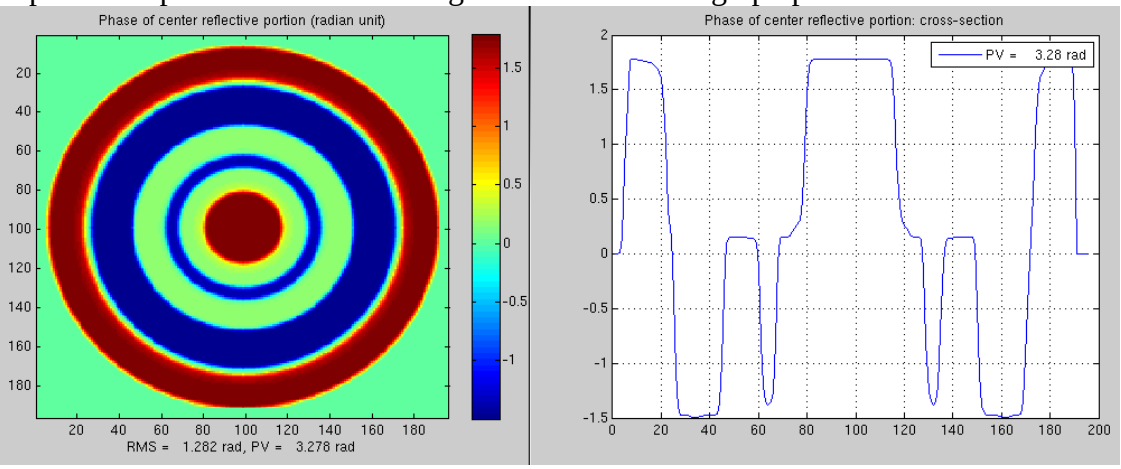

Figure 7 HLC phase profile with LOWFS phase dimple in the center

Figure 8 shows two HLC phase plate designs[3]. The bottom nickel layer serves as a reflective mirror and the coating material (MgF2 or PMGI) produces the desired phase delay modulation. Multiple reflections inside the dielectric layer affect the phase delay. The delay phase is a function of refractive index difference, profile depth/thickness, wavelength, and the incident angle. Figure 9 shows the phase and reflectivity at different wavelength.

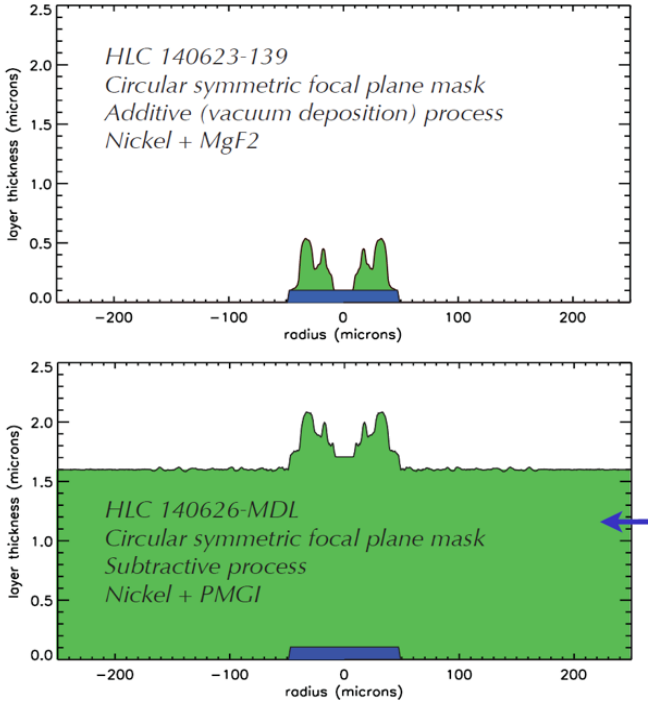

Figure 8 Two different HLC phase plate designs

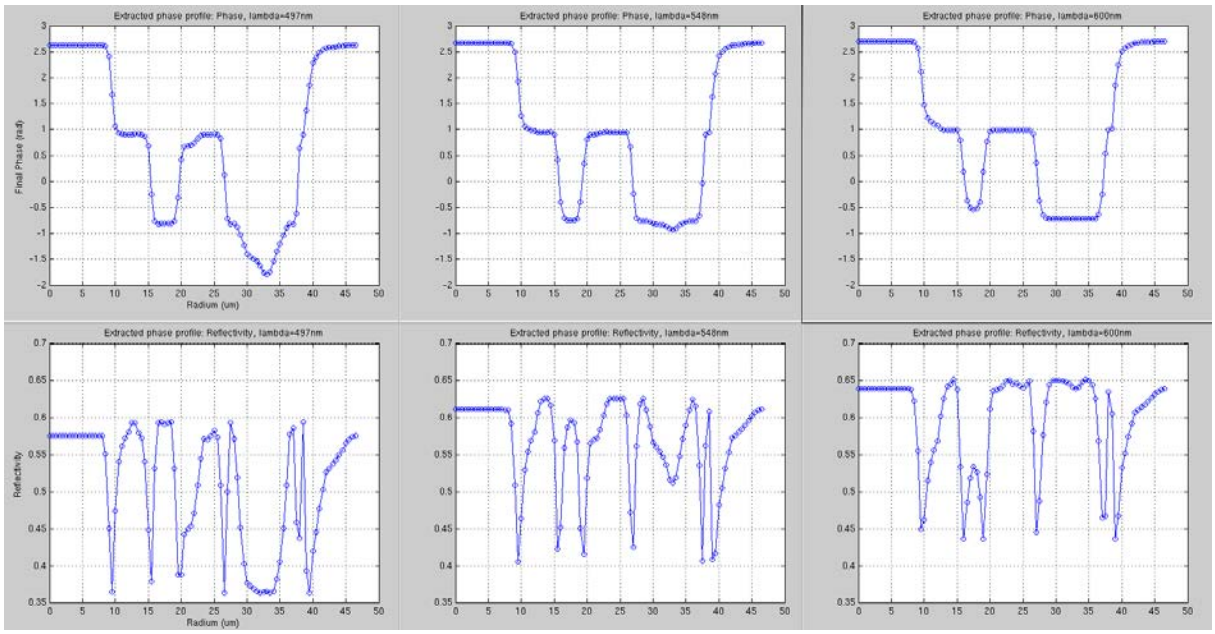

Figure 9 Delay phase and reflectivity versus wavelength

JPL micro-device lab (MDL) manufactured the HLC 140626-MDL design. Figure 10 compares the design and as-built phase plate. The modeling prediction uses the phase delay computed from this measured surface profile.

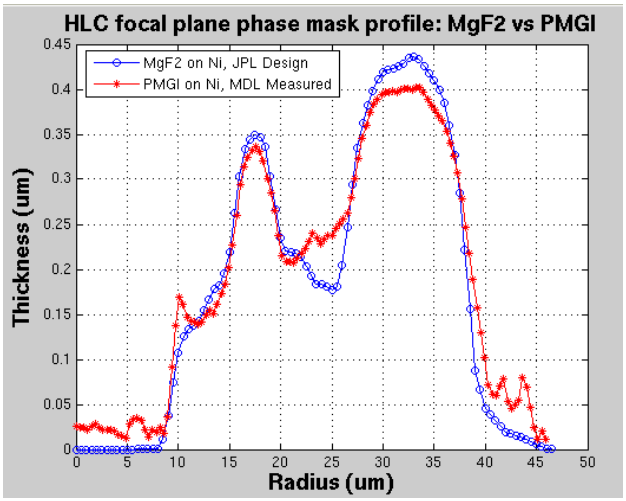

Figure 10 Comparison of HLC phase plate profiles

3.2 Testbed description

To demonstrate and evaluate the performance of LOWFS/C with HLC and SPC coronagraph modes under the representative WFIRST environment, we designed an Optical Telescope Assembly (OTA) Simulator to inject the expected WFIRST wavefront drift and LoS jitter into the OMC coronagraph testbed. The OTA Simulator provides a point source with adjustable brightness and spectral bandwidth. It also mimics pupil shape of the obscured 2.4 meter WFIRST telescope. Besides OTA Simulator, the LOWFS/C testbed consists of the Zernike wavefront sensor (ZWFS) with a commercial CCD camera running at 780 Hz frame rate, the Fast Steering Mirror (FSM) for LoS jitter correction, and the focusing mirror (FM).

Figure 11 shows the optical layout and functions of the OTA Simulator and LOWFS/C testbed. The OTA Simulator uses a fiber illuminated pinhole as the star. The light from the pinhole is collimated by a miniature telescope with the scaled down WFIRST telescope primary mirror (PM) and secondary mirror (SM). A pupil mask behind the secondary mirror support creates the WFIRST pupil shape which has the SM obscuration and the shadows of the SM supporting struts. This pupil is then relayed by a pair of off-axis parabolas (OAP 1 and 2) to the Jitter Mirror (JM) which is a small flat mirror on a PZT tilt stage with strain gauges. It injects high frequency LoS jitter into the system. After the JM, another pair of OAPs (OAP 3 and 4) collimate the beam and form another pupil just outside the OTA Simulator sub-bench for interface with the LOWFS/C testbed optics. In the OTA Simulator, 6 degrees of freedoms PZT actuators on the SM and OAP2 simulate the WFIRST low order WFE drift. The LOWFS/C testbed starts with the FSM. The following OAP focuses beam on the ZWFS mask. The beam is folded by a flat mirror on a linear stage acting to adjust focus. The ZWFS light reflects from a focal plane mask and is collected and collimated by Lens 1 and re-imaged to LOWFS/C CCD camera by Lenses 2 and 3. They form a pupil image of 16x16 pixels on the LOWFS/C CCD camera.

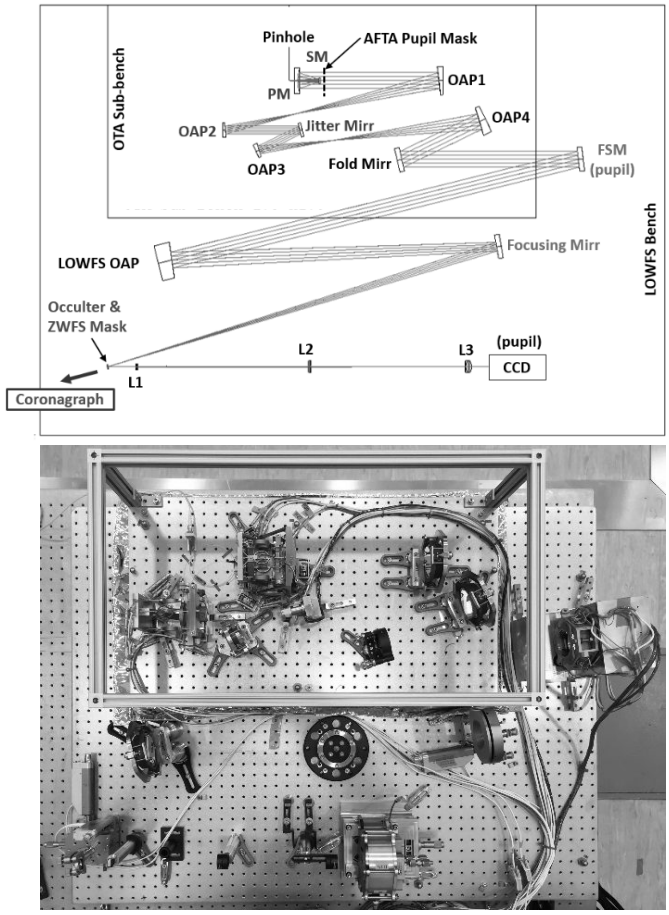

Figure 11 The OTA Simulator and the LOWFS/C testbed. The plot on the top is the optical layout, and picture on the bottom is the testbed after integration, oriented the same way as layout.

3.3 Preliminary measurement vs modeling

Figure 12 compares the measured and modelled beam spot (at the CCD detector). Overall, the beam spot patterns are similar. The center portion of the measured data shows some modulation of the spider shape of the pupil. This ghost image of pupil mask is coming from the ~4%

reflection of the phase plate glass substrate (outer zones). The AR coating was later applied and phase masks for different configurations (HLC, SPC, simple phase dimple) with various design parameters, such as phase depth and diameter, were designed and manufactured. The detailed measurement versus model comparison of these masks will be covered in an upcoming paper.

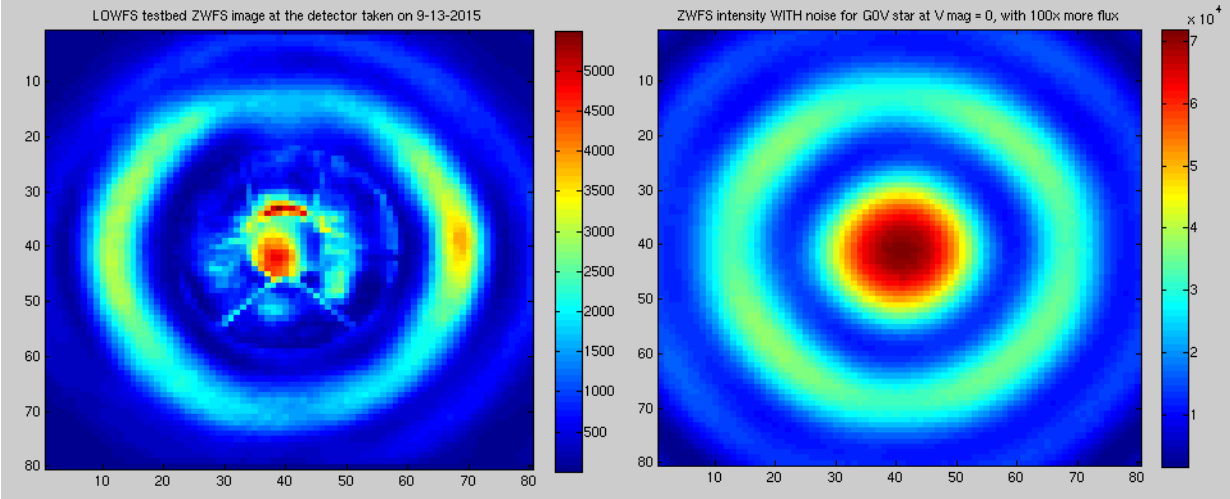

Figure 12 Measured beam spot at the detector(left) and modeling prediction(right).

4. CONCLUSION

The WFIRST coronagraph requires a low order wavefront sensing and control subsystem to maintain the coronagraph's contrast stability. A Zernike phase contrast wavefront sensor is selected to sense the low order wavefront drift and line-of-sight jitter using the starlight rejected by the coronagraph's focal plane mask. A suite of ZWFS models have been developed, thoroughly tested, and used for sensitivity studies on various noises and perturbations. The modeling analysis and the preliminary lab test suggests that ZWFS sensor is capable of detecting sub milliarcsecond tilt, as needed for WFIRST coronagraph to meet its science requirements.

ACKNOWLEDGEMENT

This research was carried out at the Jet Propulsion Laboratory, California Institute of Technology, under contract with the National Aeronautics and Space Administration (NASA).

REFERENCES

1. X.Wang, S.Fang, K.Wallace, "*Zernike wavefront sensor modeling development for LOWFS on WFIRST-AFTA*", *Proc. SPIE* **9605**, 960528-14 (2015)
2. R. Soummer, etal, "*Fast computation of Lyot-style coronagraph propagation*", Optics Express, Vol. 15, No. 24 15935, (2007)
3. J. Trauger, etal, "*Hybrid Lyot Coronagraph for WFIRST-AFTA: coronagraph design and performance metrics*", *JATIS*, Vol 2, #1, 011013, 2016